Zirconia nanopowder synthesis via detonation of trinitrotoluene

Pierre Gibot, Loic Vidal, Lydia Laffont, Julien Mory

Zirconia nanopowder synthesis via detonation of trinitrotoluene

Pierre Gibot[a,*], Loic Vidal[b], Lydia Laffont[c], Julien Mory[d]

[a] Laboratoire Nanomatériaux pour Systèmes Sous Sollicitations Extrêmes (NS3E) UMR 3208 ISL/CNRS/UNISTRA, Institut Franco-allemand de Recherches de Saint-Louis (ISL), 5 Rue du Général Cassagnou, BP70034, 68301, Saint Louis, France
[b] Institut de Science des Matériaux de Mulhouse (IS2M) UMR 7361 CNRS/UHA, 15 Rue Jean Starcky, BP2488, 68057, Mulhouse, France
[c] CIRIMAT, Université de Toulouse, CNRS, INP-ENSIACET, 4 Allée Emile Monso, BP 44362, 31030, Toulouse Cedex 4, France
[d] Laboratoire Physique des Chocs et Détonique, ISL, 5 Rue du Général Cassagnou, BP70034, 68301, Saint Louis, France

Keywords:
Powders
Detonation synthesis
ZrO_2
Transition metal oxides
Nanoparticles

A B S T R A C T

Zirconium (IV) oxide nanopowder was successfully synthesized through the detonation of a mixture composed of 2,4,6 trinitrotoluene (TNT, $C_7H_5N_3O_6$) and zirconium sulfate tetrahydrate ($Zr(SO_4)_2{\cdot}4H_2O$) as the energetic material and ceramic precursor, respectively. TNT, one of the most popular explosives, is a secondary energetic molecule and exhibits high stability and low sensitivity toward external stresses, making its handling safe. After detonation of the energetic material/ceramic precursor mixture and purification of the detonation soot, a crystallized zirconium oxide (ZrO_2) powder composed of nanosized particles with a spherical morphology was produced and analysed by the usual characterization techniques (X-ray diffraction, Fourier transform infrared spectroscopy, transmission electron microscopy and nitrogen physisorption). The reaction mechanism, considering the thermochemical aspect of the explosive, is offered. This approach could provide promising opportunities for the synthesis of various nano-sized oxide ceramic powders.

1. Introduction

Zirconium (IV) oxide is an outstanding refractory ceramic material since it exhibits very interesting physicochemical properties, such as high melting (2700 °C) and boiling points (> 4500 °C) and high thermal and chemical inertias, particularly under alkali conditions [1]. The crystallographic structure of zirconium oxide material can be described as transitioning between three well-known crystallographic phases [2]: the monoclinic phase ($P2_1/c$ space group) up to 1170 °C, the intermediate tetragonal phase ($P4_2/nmc$ space group) from 1170 to 2370 °C and the cubic phase ($Fm3m$ space group) from 2370 °C to the melting point. These last two crystal structures can be stabilized at room temperature by the addition of a weak molar percent of calcium oxide (CaO), cerium (IV) oxide (CeO_2), magnesium oxide (MgO) or yttrium oxide (Y_2O_3) [3]. The high diversity of the physico-chemical properties and crystalline structures of this ceramic material makes it promising for a large number of applications in many areas, such as fuel cells [4], sensors [5], bioceramics [6] and catalysts [7].

To satisfy these numerous applications, synthesizing a tunable zirconium (IV) oxide material that exhibits distinct physical surface properties (i.e., particle size, specific surface area, and porosity) or particles with various morphologies has become paramount. Thus, as a large number of these properties strongly depend of the synthesis conditions, many processes have been developed, including sol-gel without ultrasound assistance [8,9], coprecipitation [10,11], hydrothermal [12], mechanochemical [13], microwave [14], Pechini [15] and combustion methods [16]. More recently, an unconventional dynamic method based on the detonation of highly energetic materials (EM) or explosives to generate precursors for powder preparation has been published in the literature. This method combines high temperatures (> 1000 °C) and pressures (> GPa) for short times, thus producing (metastable) materials at nanoscales. The nanometric dimensions of the materials are assured by a cooling bath surrounding the energetic charge. The first example of successful detonation synthesis was reported for nanodiamonds using a mixture of two common secondary explosives, 2,4,6 trinitrotoluene (TNT) and 1,3,5 trinitro-1,3,5-triazine (RDX) [17]. From these initial results, some researchers have used RDX and ammonium nitrate (NH_4NO_3), an inorganic energetic molecule; or a mixture of both as the detonation source for producing single (Al_2O_3, ZrO_2, B_2O_3, TiO_2, ZnO, CeO_2) [18–25] or mixed oxide ceramics (Gd_2O_3/CeO_2, $LiMn_2O_4$, $MnFe_2O_4$, $SrAl_2O_4$) [26–29]. The ammonium nitrate-based explosive emulsion approach was patented by Refs. [30,31], and Innovnano markets an as-detonated yttria-stabilized zirconia material [30–32]. These authors claim many advantages regarding the detonation method, such the synthesis of a pure material consisting of particles with a spherical morphology and of nanometric

* Corresponding author.
E-mail address: pierre.gibot@isl.eu (P. Gibot).

https://doi.org/10.1016/j.ceramint.2020.07.182

size. For example, Bukaemskii synthesized a nanosized zirconia powder from a mixture of zirconium hydroxide ($Zr(OH)_x$) and RDX as the zirconium precursor and explosive molecule, respectively [33]. Cubic 5-6 nm-sized ZrO_2 particles were successfully produced without the assistance of a stabilizing compound, as used in previous studies. Recently, non-oxide ceramics have also be prepared via the explosive route [34–36]. For example, Örnek et al. have successfully demonstrated the synthesis of nanoscale metastable boron nitride phases (w-BN and e-BN) from the detonation of a hexagonal boron nitride phase (h-BN) mixed with an explosive emulsion [34,35]. Langenderfer and co-workers have synthesized silicon carbide nanoparticles by submitted a pre-ceramic polymer (polycarbosilane) to the high pressures and temperatures generated by the detonation of a 2,4,6-trinitrotoluene and 1,3,5-trinitro-1,3,5-triazine energetic mixture [36]. Succinctly, the literature cited above evidences the high potential of this approach given the possibility of producing nano-sized materials, of stabilizing metastable phases and that for different kinds of materials.

Herein, a zirconium (IV) oxide nanopowder was detonation-synthesized using a mixture of 2,4,6 trinitrotoluene (TNT) and zirconium (IV) sulfate tetrahydrate as the explosive substance and zirconium source, respectively. TNT has the advantage of being less sensitive to mechanical stimuli than RDX, thus contributing to operator safety during the handling of these explosive compositions [37]. For example, the impact and friction sensitivities of TNT are 15 J and 353 N, respectively, compared to 7.4 J and 120 N for RDX. Finally, the as-detonated product was submitted to a series of analyses for characterization.

2. Experimental section

Zirconium sulfate tetrahydrate ($Zr(SO_4)_2{\cdot}4H_2O$, 99%) was purchased from Alfa Aesar. The energetic mixture of 2,4,6 trinitrotoluene or 2-methyl-1,3,5-trinitrobenzene (TNT, $C_6H_2(NO_2)_3CH_3$) and 1,3,5-trinitro-2-[2-(2,4,6-trinitrophenyl)-ethenyl] benzene or hexanitrostilbene (HNS, $((NO_2)_3C_6H_2CH)_2$) (99.65/0.35 wt%) was provided by Titanobel. Estane 5703, a polyester type thermoplastic polyurethane, was obtained from Lubrizol Advanced Materials, Inc. Hydrochloric acid (37%) was obtained from Prolabo.

2.1. Preparation of the zirconium-based energetic charge

The zirconium sulfate hydrate material was covered by an Estane 5703 polymer layer using a dissolution/precipitation synthesis method. Using vigorous stirring (600 rpm), 1.54 g of Estane 5703 was dissolved in 200 mL of acetone. Then, 29.64 g of zirconium salt was dispersed in the solution, and the mixture was stirred to obtain a homogeneous solution. Then, 460 mL of heptane was added (the first 280 mL added drop-by-drop) to the previous solution and maintained under stirring conditions to precipitate the polymer. Acetone was removed using a rotating evaporator (50 °C, 100 mbars), and the $Zr(SO_4)_2{\cdot}4H_2O$/Estane 5703 granules (95/5 wt ratio) were separated by filtration followed by washing with heptane. The $Zr(SO_4)_2{\cdot}4H_2O$/Estane 5703 powder was mixed with the 2,4,6 trinitrotoluene/1,3,5-trinitro-2-[2-(2,4,6-trinitrophenyl)-ethenyl] benzene explosive substance at a 10:90 wt ratio using a Turbula mixer (model T2A – W.A. Bachofen) at 23 rpm for 20 min. The mixture was preheated at 70 °C (30 min) and pressed at 765 bars for 10 min. Cooling was performed at 230 bars to 8 °C before releasing the mould. Cylindrical pellets (L = 50 mm, Ø = 45 mm) with a density of 1.703 ± 0.002, corresponding to 98% of the theoretical maximum density (TMD), were thus obtained. Two pellets were glued, placed in a plastic bag containing demineralized water and hung in the centre of a detonation chamber. Water was used to cool the detonation products extremely rapidly. A booster (graphite/wax/1,3,5-trinitro-1,3,5-triazinane secondary explosive 0.5/5/94.5 wt%, 55 g, Ø = 28.4 mm, L = 57.5 mm) and an electric initiator (SA4000, Davey Bickford) were used to complete the energetic train. After detonation, the soot was filtered to remove plastic and metal fragments, washed with 2 mol/L hydrochloric acid to dissolve the rust from the detonation chamber and calcined at 700 °C for 1 h to oxidize the carbonaceous products of the TNT detonation and polypropylene tube combustion. The oxide ceramic yield was ~35%.

2.2. Characterization techniques

X-ray powder diffraction (XRD) was recorded on a D8 Advance diffractometer (Bruker, Billerica, MA, USA) using Cu-Kα radiation (λ = 1.54056 Å) equipped with a Lynxeye detector and operating at 40 kV and 40 mA in the range 2θ = 20–80° with a 2θ step size of 0.02°. Fourier Transform Infra-Red (FT-IR) spectroscopy analysis of the sample was conducted using a Bruker Tensor 27 spectrometer. The spectrum was recorded in the transmission mode (KBr pellets) with a wavenumber range of 4000–450 cm^{-1} and by superposing 16 scans. The resolution was fixed at 4 cm^{-1}. The structure and microstructure of the product was determined using a JEM 2100F transmission electron microscope (JEOL, Tokyo, Japan) at an acceleration voltage of 200 kV and equipped with an energy dispersive spectrometer. The diffraction pattern of the investigated material was obtained using the selected area electron diffraction mode or by Fast Fourier transform of the high-resolution transmission electron microscopy images. Nitrogen sorption measurements at −196 °C were carried out on an ASAP2020 surface area analyser (Micromeritics, Norcross, GA, USA) with the sample outgassed at 200 °C under vacuum for 6 h. The specific surface area was determined according to the Brunauer–Emmett–Teller method within the 0.05–0.20 relative pressure domain. The particle size distribution of the powder, which as previously dispersed in chloroform (0.1 g/L), was determined by dynamic light scattering using a Zetasizer nanoZS apparatus (Malvern Instrument, Worcestershire, United Kingdom).

3. Results and discussion

The XRD pattern of the product synthesized by the detonation of a TNT/$Zr(SO_4)_2{\cdot}4H_2O$ (90/10 wt%) energetic charge is displayed in Fig. 1 (top). All the diffraction peaks could be assigned to the single zirconium (IV) oxide phase (ZrO_2) except for the two thick and low intensity peaks located at ~21° and ~26–27°, which were assigned to an impurity from the white paint covering the inner wall of the detonation tank (Fig. 1 top, symbol star). The impurity was identified as silica in quartz form (JCPDS 01-087-2096). Note that a sand blasting operation is planned in the near future to remove this impurity. Regarding the zirconia phase, both polymorphs were detected, including the monoclinic and tetragonal structures described as $P2_1/a$ and $P4_2/nmc$ space groups, and were identified by the JCPDS card No 37-1484 and No 72-7115, respectively. Taking into account the relative intensity of the diffraction peaks described in both crystallographic reference cards, a preferential orientation/growth of the crystallite was observed at 2Θ = 35–36°, which may correspond to the (002) and (110) Miller planes of the monoclinic and tetragonal phases, respectively. To date, the reaction mechanism is not yet well-understood, and an investigation is in progress.

The volume percent (V_m) of the monoclinic structure was determined using formula (1) by Schmid et al. [38] as given below:

$$V_m = \frac{1.311.\ X_m}{1 + 0.311.\ X_m} \quad (1)$$

where X_m, the ratio of integrated intensities (noted I) of specific (hkl) diffraction peaks, was specified by formula (2):

$$X_m = \frac{I_{m(-111)} + I_{m(111)}}{I_{m(-111)} + I_{m(111)} + I_{t(101)}} \quad (2)$$

A volume fraction of ~52% monoclinic phase was calculated (45% of X_m weight fraction), in the ZrO_2 powder.

Fig. 2 shows the FTIR spectrum of the product synthesized by the

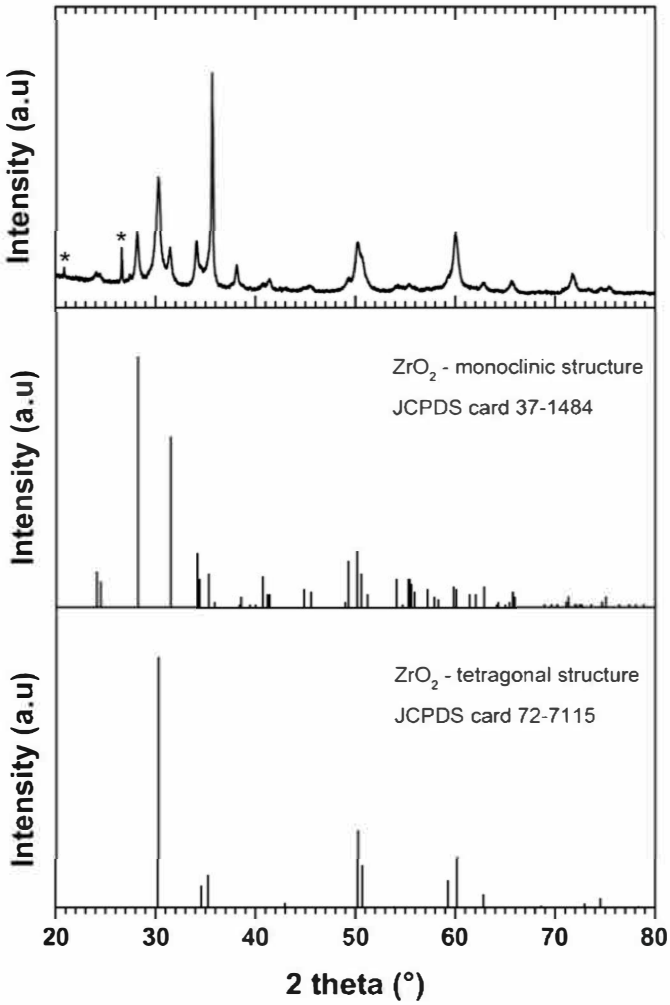

Fig. 1. XRD patterns of the zirconium (IV) oxide sample (ZrO_2) synthesized via detonation of a 2,4,6 trinitrotoluene/zirconium-salt (90/10 wt%) explosive charge. Monoclinic and tetragonal structures are given for the XRD peak attribution.

detonation of the TNT/$Zr(SO_4)_2{\cdot}4H_2O$ (90/10 wt%) energetic charge, magnified on the 500–1000 cm^{-1} domain characterizing the metal-oxygen bonds vibration. The wavenumbers identifying each infrared vibration band are reported on the spectrum. The intense vibration band at 505 cm^{-1} was assigned to the Zr–O bond vibration in the tetragonal structure, while the bands at 578 and 744 cm^{-1} were correlated to zirconia material in the monoclinic phase [39]. This result supports the previous structural result (XRD) that showed the coexistence of both zirconia phases. An overview of the spectrum; i.e. over 1000 cm^{-1} is shown on Supporting information. The different visible vibration bands were associated with the vibrational modes of hydroxyl groups (–OH) or water molecules, both physisorbed on the surface of the material. Traces of the silica impurity were also observed.

The as-detonated zirconia powder was imaged by transmission electron microscopy (TEM) and high resolution (HR)-TEM analysis in order to reveal the morphology, structure and crystalline degree of the particles. Representative views are displayed in Fig. 3. At low magnification, the TEM bright-field images clearly showed highly agglomerated particles exhibiting a nanometric dimension (Fig. 3A). At an intermediate magnification, as shown in Fig. 3B, the nanoparticles adopted a spherical morphology with a shape factor close to one. The particle dimensions were definitively at the nanoscale, and the particle size distribution appeared to be narrow with the main size range of approximately 25–30 nm. In the insert in Fig. 3B, a selected area electron diffraction pattern (SAED) obtained on the nanoparticles confirmed the crystallinity of the powder due to the presence of rings. The HRTEM image shown in Fig. 3C highlights the diffraction planes present in a particle. The Fast Fourier transform (insert of Fig. 3C) of the HRTEM image of one nanoparticle is indexed using the monoclinic structure with a space group $P2_1/a$ corresponding to ZrO_2 zirconia.

Nitrogen adsorption analysis provided textural properties data for the as-detonated ZrO_2 sample. In particular, the specific surface area (S), taking into account the Brunauer-Emmett-Teller (BET) model, was determined to be ~32 m^2/g. Assuming the zirconia powder was

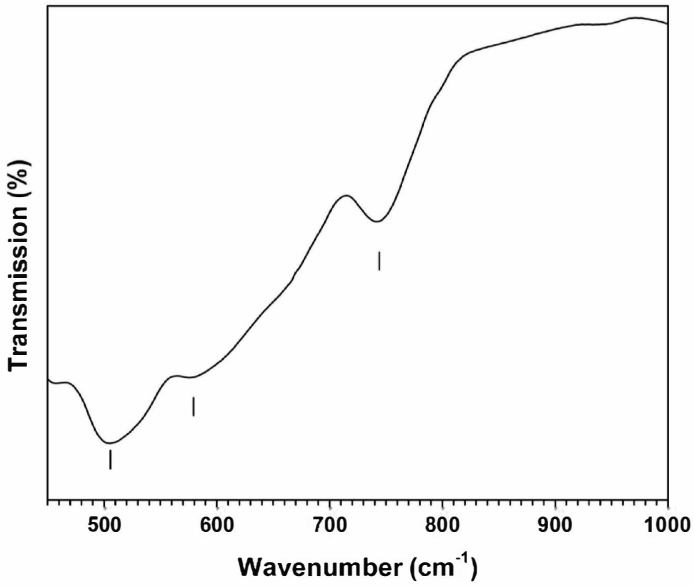

Fig. 2. FTIR spectrum of the ZrO_2 powder synthesized via detonation of a 2,4,6 trinitrotoluene/zirconium-salt (90/10 wt%) explosive charge.

composed of monodisperse dense spherical particles and knowing its density (ρ = 5890 kg/m^3), the average particle size (∅) was estimated using the following formula (3) [40]:

$$\varnothing = \frac{6}{\rho \times S_{BET}} \quad (3)$$

The average particle size was thus calculated to be approximately 32 nm, which is in good agreement with the trend observed by the microscopic analysis.

Based on the results determined above, a discussion is attempted in order to elucidate some points regarding the present synthesis method, namely the composition of the detonation soot, the particles size as well as the structure of the detonation products.

The detonation soot's composition is dependent on the reaction mechanism. The chemical decomposition mechanism taking place during the zirconia ceramic detonation synthesis was quite complex since the initial explosive mixture consisted of several ingredients, including explosive substances, such as 2,4,6 trinitrotoluene (TNT, $C_7H_5N_3O_6$) and hexanitrostilbene (HNS, $C_{14}H_6N_6O_{12}$), and the inert zirconium salt ($Zr(SO_4)_2{\cdot}4H_2O$). Estane polymer was voluntary discarded to simplify the reactive system. To investigate the detonation process, the decomposition reaction of the mixture may consider the sum of the decomposition chemical reactions of each ingredient independently. Based on the chemistry of the explosives, including the thermochemical aspect [41], the decomposition reaction of both explosive molecules, TNT and HNS, considering the Kistiakowsky-Wilson rules (the oxygen balance of TNT and HNS are much lower; i.e., −74.00 and −67.60 wt%, respectively), could be described by reactions (4) and (5) below:

$$2C_7H_5N_3O_{6(s)} \rightarrow 3N_{2(g)} + 5H_2O_{(g)} + 7CO_{(g)} + 7C_{(s)} \quad (4)$$

$$C_{14}H_6N_6O_{12(s)} \rightarrow 3N_{2(g)} + 3H_2O_{(g)} + 9CO_{(g)} + 5C_{(s)} \quad (5)$$

Note that negative oxygen balances will lead to the formation of a carbon solid phase since the amount of oxygen within the molecules was not enough to completely oxidize the compounds considered [41]. The thermal decomposition reaction of the Zr-salt inert compound could be represented by equation (6):

$$Zr(SO_4)_2{\cdot}4H_2O_{(s)} \rightarrow ZrO_{2(s)} + 4SO_{2(g)} + 3O_{2(g)} + 4H_2O_{(g)} \quad (6)$$

Finally, the global detonation reaction could be summarized by equation (7) based on the reaction of 1 g of mixture and taking into account the weight percentage of each of the three ingredients comprising the zirconium-doped explosive mixture (89.68, 0.32 and 10 wt % for TNT, HNS and $Zr(SO_4)_2{\cdot}4H_2O$, respectively):

$$0.00395C_7H_5N_3O_{6(s)} + 0.000007C_{14}H_6N_6O_{12(s)} + 0.00028Zr(SO_4)_2{\cdot}4H_2O_{(s)} \rightarrow 0.00594N_{2(g)} + 0.01102H_2O_{(g)} + 0.01445CO_{(g)} + 0.01330C_{(s)} + 0.00028ZrO_{2(s)} + 0.00056SO_{2(g)} \quad (7)$$

Note that only carbon and zirconia solid phases were formed during the detonation, in line with the results obtained from the different characterization techniques shown previously. These two species were found in the detonation soot and were accompanied by impurities, such as iron oxide (Fe_2O_3) and silicium oxide (SiO_2), originating from the roost and paint covering the inner wall of the detonation chamber. Most of the impurities were discarded during the purification process.

Regarding the particles size of the as-detonated zirconia powder, the detonation approach is known to generate high pressures (GPa) and temperatures (> 1000 °C) that are suitable to the gasification of the precursors and the formation of crystalline phases during the subsequent condensation step [19,30–33,37,41]. More, the extremely high cooling rate of the detonation gaseous products, estimated as high as 10^9 °C/s due to the rapid expansion of the chemical species, impedes the growth of particles produced and consequently leads to the formation of materials of nanoscale dimension [21–36]. The use of water to cool down the detonation products (see Experimental section) efficiently also acts to stop the growth of condensed species and thus controls the particles size in the nanoscale.

Concerning the structure of the as-detonated zirconia powder, monoclinic and tetragonal phases were prepared. The metastable cubic structure was not identified. Based on the work of Bukaemskii [33], the cubic phase is favoured for the smallest particles due to a layer-by-layer growth model where surface layers are preferentially made of high-

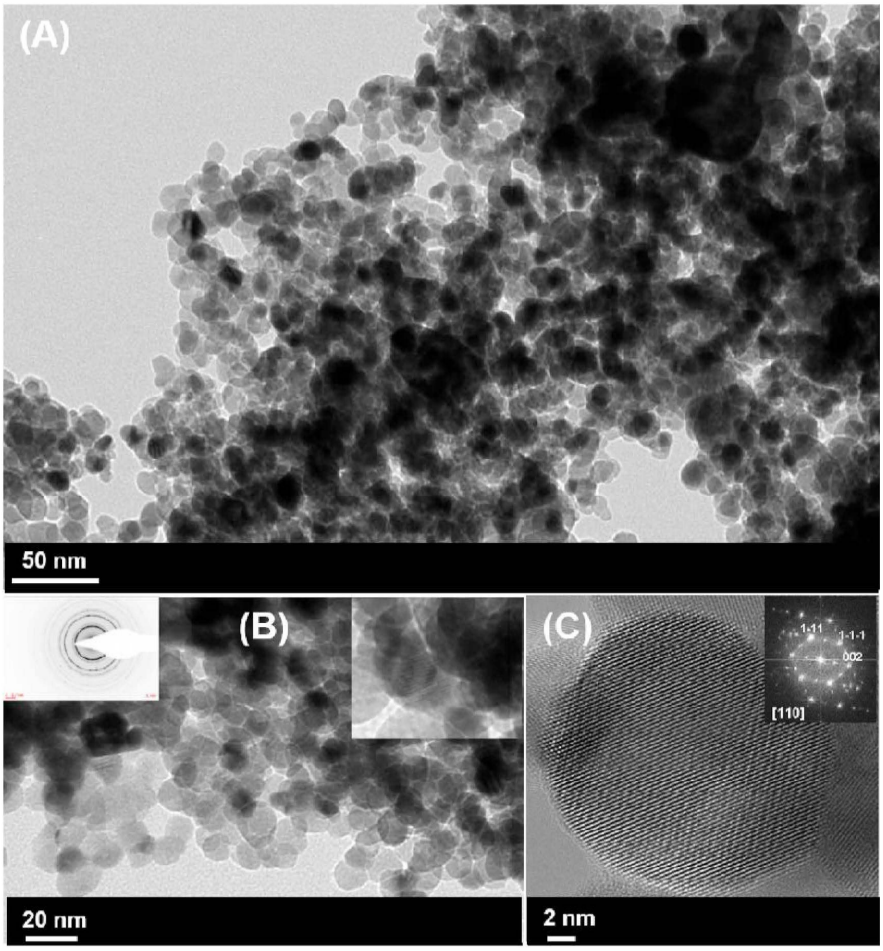

Fig. 3. (A, B) TEM and (C) high resolution (HR) TEM images of the ZrO_2 powder synthesized via detonation of a 2,4,6 trinitrotoluene/zirconium-salt (90/10 wt%) explosive charge.

temperature phases. Particles smaller than ~10 nm would adopt a cubic structure moving gradually towards the tetragonal and finally the monoclinic phases as the particle growths. As, in the present work, the as-detonated ZrO_2 particles exhibit a particle size ranging from 25 to 30 nm, the cubic structure was not favoured. Now, regarding the formation of both monoclinic and tetragonal phases, it can be explain by a mitigation of the shock wave during its dissipation in all the volume of the detonation chamber [33]. It can be speculate that this mitigation leads to the coexistence of reaction zones where pressures and temperatures are different. Highest pressures and highest temperatures domains (close to the central axis of the cylindrical charge) would promote the formation of the metastable tetragonal phase at the expense of the monoclinic one which might rather originate from the zone located at the edge of the charge [33–35]. Currently, it has not be possible to distinguish the crystalline structure of the ZrO_2 material as function of the particles size.

4. Conclusion

In summary, a zirconia nanopowder (ZrO_2) was synthesized via a detonation process using 2,4,6 trinitrotoluene (TNT) as the high energetic molecule mixed with zirconium sulfate. TNT is one of the energetic materials with the lowest sensitivity compared to other high explosives that can be used in such a process, and therefore, it is seen as a promising compound for future development. In addition, as the melting point of TNT is low (80.8 °C), it can be used in melting or casting processes to lead to more homogeneous explosive/ceramic precursor mixtures. In the present work, purified soot was composed of ZrO_2 particles exhibiting well-defined microstructural properties (spherical morphology, nanoscale particles size, narrow particles size distribution). However, the simultaneous synthesis of two zirconia polymorphs could be a disadvantage for many applications, which may be able to be overcome by adding stabilizing ingredients, such as yttrium, cerium, or calcium oxides, in the initial detonative mixture. Successful synthesis of mixed oxides has been demonstrated in the previous literature. Finally, the present investigation confirmed that explosive synthesis routes are efficient and suitable for producing nanosized ceramics powders.

Declaration of competing interest

The authors declare that they have no known competing financial interests or personal relationships that could have appeared to influence the work reported in this paper.

Acknowledgements

The French National Centre for Scientific Research (CNRS), French German Research Institute of Saint-Louis (ISL, Saint-Louis, France) and University of Strasbourg (UNISTRA, Strasbourg, France) are acknowledged by the authors for funding. The authors thank E. Fousson (ISL, Saint-Louis) and D. Spitzer (director of NS3E laboratory, Saint-Louis) for the help in the explosion experiments and the incentives to develop this research topic, respectively.

Appendix A. Supplementary data

Supplementary data to this article can be found online at https://doi.org/10.1016/j.ceramint.2020.07.182.

References

[1] Handbook of Chemistry and Physics, 84th ed., The Chemical Rubber Co, Ohio, 2003-2004.
[2] G. Beranger, J. Favergeon, G. Moulin, Zircone-Céramique Fonctionnelle, Techniques de l'ingénieur, 2008.
[3] J.M. Haussonne, C. Carry, P. Bowen, J. Barton, Céramiques, et al., Principes et Techniques d'élaboration, first ed., Presses polytechniques et universitaires romandes, Lausanne, 2005.
[4] B.C.H. Steele, A. Heinzel, Materials for fuel-cell technologies, Nature 414 (2001) 345–352.
[5] S.A. Ghom, C. Zamani, S. Nazarpour, T. Andreu, J.R. Morante, Oxygen sensing with mesoporous ceria–zirconia solid solutions, Sens. Actuators B. 140 (2009) 216–221.
[6] C. Piconi, G. Maccauro, Zirconia as a ceramic biomaterial, Biomaterials 20 (1999) 1–25.
[7] Y. Li, D. He, Z. Cheng, C. Su, J. Li, Q. Zhu, Effect of calcium salts on isosynthesis over ZrO_2 catalysts, J. Mol. Catal. A: Chem. 175 (2001) 267–275.
[8] J. Yan, X. Li, S. Cheng, Y. Ke, X. Liang, Facile synthesis of titania–zirconia monodisperse microspheres and application for phosphopeptides enrichment, Chem Commun (2009) 2929–2931.
[9] J. Judes, V. Kamaraj, Sol-gel preparation and characterization of ceria stabilized zirconia minispheres, J. Sol. Gel Sci. Technol. 49 (2009) 159–165.
[10] H. Chen, A. Yin, X. Guo, W. Dai, K. Fan, Sodium hydroxide-sodium oxalate-assisted co-precipitation of highly active and stable Cu/ZrO_2 catalyst in the partial oxidation of methanol to hydrogen, Catal. Lett. 131 (2009) 632–642.
[11] M. Dechamps, B. Djuricic, S. Pickering, Structure of zirconia prepared by homogeneous precipitation, J. Am. Ceram. Soc. 78 (1995) 2873–2880.
[12] T.M. Arantes, G.P. Mambrini, D.G. Stroppa, E.R. Leite, E. Longo, A.J. Ramirez, E.R. Camargo, Stable colloidal suspensions of nanostructured zirconium oxide synthesized by hydrothermal process, J. Nanopart. Res. 12 (2010) 3105–3110.
[13] A. Dodd, P. McCormick, Synthesis of nanocrystalline ZrO_2 powders by mechanochemical reaction of $ZrCl_4$ with LiOH, J. Eur. Ceram. Soc. 22 (2002) 1823–1829.
[14] Y.T. Moon, D.K. Kim, C.H. Kim, Preparation of monodisperse ZrO_2 by the microwave heating of zirconyl chloride solutions, J. Am. Ceram. Soc. 78 (1995) 1103–1106.
[15] C. Lin, C. Zhang, J. Lin, Phase transformation and photoluminescence properties of nanocrystalline ZrO_2 powders prepared via the Pechini-type sol-gel process, J. Phys. Chem. C 111 (2007) 3300–3307.
[16] I.O. Fabregas, D.G. Lamas, Parametric study of the gel-combustion synthesis of nanocrystalline ZrO_2-based powders, Powder Technol. 214 (2011) 218–228.
[17] V.N. Mochalin, O. Shenderova, D. Ho, Y. Gogotsi, The properties and applications of nanodiamonds, Nat. Nanotechnol. 7 (2012) 11–23.
[18] S. Cudzilo, A. Maranda, J. Nowaczewski, R. Trebinski, W.A. Trzcinski, Detonative synthesis of inorganic compounds, J. Mater. Sci. Lett. 9 (2000) 1997–2000.
[19] A.A. Bukaemskii, Explosive synthesis of ultra-disperse aluminium oxide in an oxygen-containing medium, Combust. Explos. Shock Waves 37 (2001) 594–599.
[20] R.Y. Li, X.J. Li, H.H. Yan, J. Peng, Experimental investigations of the controlled explosive synthesis of ultrafine Al_2O_3, Combust. Explos. Shock Waves 49 (2013) 105–108.
[21] Y. Qu, X. Li, X. Wang, D. Liu, Detonation synthesis of nanosized titanium oxide powders, Nanotechnology 18 (2007) 205602–205607.
[22] Y.D. Qu, X.J. Li, H.H. Yan, X. Ouyang, Selective synthesis of TiO_2 nanopowders, Glass Phys. Chem. 34 (2008) 637–639.
[23] H. Yan, T. Zhao, X. Li, B. Zhao, Slurry explosive detonation synthesis and characterization of 10 nm TiO_2, Ceram. Int. 42 (2016) 14862–14866.
[24] X. Xie, X. Li, H. Yan, Detonation synthesis of zinc oxide nanometer powders, Mater. Lett. 60 (2006) 3149–3152.
[25] Z.W. Han, S. Xu, L.F. Xie, Y.C. Han, Study on the application of emulsion explosives in synthesizing nanostructured ceria, Combust. Explos. Shock Waves 50 (2014) 477–482.
[26] O. Vasylkiv, Y. Sakka, Nanoexplosion synthesis of multimetal oxide ceramic nanopowders, Nano Lett. 5 (2005) 2598–2604.
[27] X. Xie, X. Li, Z. Zhao, H. Wu, Y. Qu, W. Huang, Growth and morphology of nanometer $LiMn_2O_4$ powder, Powder Technol. 169 (2006) 143–146.
[28] X.H. Wang, X.J. Li, H.H. Yan, L. Xue, Y.D. Qu, G.L. Sun, Nano-$MnFe_2O_4$ powder synthesis by detonation of emulsion explosive, Appl. Phys. A. 90 (2008) 417–422.
[29] X. Li, Y. Qu, X. Xie, Z. Wang, R. Li, Preparation of $SrAl_2O_4$: Eu^{2+}, Dy^{3+} nanometer phosphors by detonation method, Mater. Lett. 60 (2006) 3673–3677.
[30] C. Da Silva, J. Manuel, A. Dos Santos, E. Marisa, Nanometric-sized ceramic materials, process for their synthesis and uses thereof, United States Patent 8 (557) (2013) 215.
[31] A. Dos Santos, E. Marisa, C. Da Silva, J. Manuel, C. Lagoa, A.L. Cia, Process for nanomaterial synthesis from the preparation and detonation of an emulsion, products and emulsions thereof, United States Patent 9 (115) (2015) 001.
[32] http://www.innovnano.pt/.
[33] A.A. Bukaemskii, Nanosize powder of zirconia. Explosive method of production and properties, Combust. Explos. Shock Waves 37 (2001) 481–485.
[34] M. Ornek, K.M. Reddy, C. Hwang, V. Domnich, A. Burgess, S. Pratas, J. Calado, K.Y. Sie, S.L. Miller, K.J. Hemker, R.A. Haber, Observations of explosion phase boron nitride formed by emulsion detonation synthesis, Scr. Mater. 145 (2018) 126–130.
[35] M. Ornek, C. Hwang, K.Y. Xie, S. Pratas, J. Calado, A. Burgess, V. Domnich, K.J. Hemker, R.A. Haber, Formation of metastable wurtzite phase boron nitride by emulsion detonation synthesis, J. Am. Ceram. Soc. 101 (2018) 3276–3281.
[36] M.J. Langenderfer, W.G. Fahrenholtz, S. Chertopalov, Y. Zhou, V.N. Mochalin, C.E. Johnson, Detonation synthesis of silicon carbide nanoparticles, Ceram. Int. 46 (2020) 6951–6954.
[37] R. Meyer, J. Kohler, A. Homburg, Explosives, sixth ed., Wiley-VCH, Weinheim, 2007.
[38] H.K. Schmid, Quantitative analysis of polymorphic mixes of zirconia by X-ray diffraction, J. Am. Ceram. Soc. 70 (1987) 367–376.
[39] M. Aflaki, F. Davar, Synthesis, luminescence and photocatalyst properties of zirconia nanosheets by modified Pechini method, J. Molecular Liquids 221 (2016) 1071–1079.
[40] S. Lowell, J.E. Shields, M.A. Thomas, M. Thommes, Characterization of Porous Solids and Powders: Surface Area, Pore Size and Density, first ed., Kluwer Academic Publishers, The Netherlands, 2004.
[41] J. Akhavan, The Chemistry of Explosives, second ed., Royal Society of Chemistry, United Kingdom, 2004.